J Electr Eng Technol Vol. 7, No. 6: 918-925, 2012
http://dx.doi.org/10.5370/JEET.2012.7.6.918

ISSN(Print) 1975-0102
ISSN(Online) 2093-7423

Performance Improvement of Grid-Connected Inverter Systems under Unbalanced and Distorted Grid Voltage by Using a PR Controller

Jong-Hyun Lee*, Hae-Gwang Jeong* and Kyo-Beum Lee†

Abstract – This paper proposes a control method for grid-connected inverter systems under unbalanced and distorted grid voltage. The proposed method can reduce the power ripple caused by the unbalanced condition and compensate for the low-order harmonics of the output currents caused by the distortion of grid voltage. To reduce the power ripple, our method replaces the two conventional PI controllers with one PR controllers in the stationary frame. PR controllers can implement selective harmonic compensation without excessive computational requirements; the use of these controllers simplifies the method. Both the simulated and experimental results agree well with the theoretical analysis.

Keywords: Grid connected inverter, PI controller, PR (Proportional Resonant) controller, Unbalanced and distorted grid voltage

1. Introduction

Global warming is one of the greatest challenges facing humanity today. It can be attributed to the cars and power plants using fossil fuels such as gasoline and natural gases [1-3].

For this reason, the contribution of renewable power sources in power generation is becoming more and more important. The inverter system is the most commonly used topology for connecting green power sources to the utility grid. The grid-connected inverter has been studied because of the importance of a distributed-power-system connection to the grid in the field of renewable energy [4–6]. Grid-connected generation systems need harmonic compensation, control of unbalanced current, an improved power factor, and anti-islanding methods. In particular, nonlinear loads at the point of common coupling lead to imbalance and low-order harmonics such as the third, fifth, and seventh harmonics in the grid voltage. These cause the grid voltage to be unbalanced and distorted into a non-sinusoidal wave.

To solve these problems, the rotating synchronous-frame proportional-integral (PI) controller is used in three-phase inverters to obtain a zero steady-state error [7]. However, this controller usually requires multiple frame transformations, and it can be difficult to implement using a low-cost digital signal processor (DSP) [8]. Thus, using PI controllers complicates the system. Specifically, many uncomfortable axis conversions are necessary because of the number of low-order harmonics that must be eliminated by the PI controller.

† Corresponding Author: Department of Electrical and Computer Engineering, Ajou University, Korea. (kyl@ajou.ac.kr)
* Department of Electrical and Computer Engineering, Ajou University, Korea. (yohann53@naver.com, lite88@ajou.ac.kr)
Received: December 30, 2011; Accepted: June 1, 2012

This paper proposes control methods that reduce the power ripple and the low-order harmonics of the output currents. The proposed PR controller in the stationary frame reduces the computational burden and has frequency response characteristics similar to those of a synchronous-frame PI controller.

2. Grid-connected inverter system

2.1 Control method of grid-connected inverter

Fig. 1 shows a grid-connected inverter system. A constant DC input voltage is needed to operate the PWM inverter. The DC-link voltage controller supplies power to the PWM inverter, ensuring that V_{dc} is constant; C_{dc} maintains the magnitude of V_{dc}.

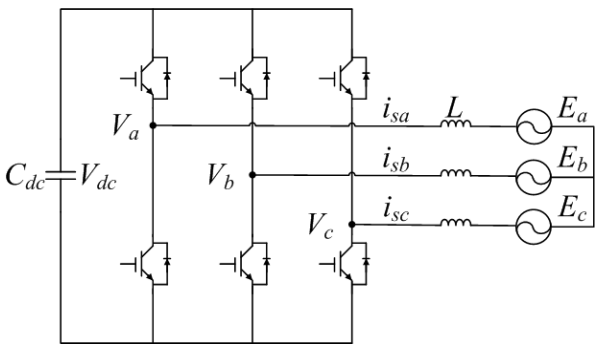

Fig. 1. Grid-connected inverter system.

To link the power system to the grid, we must match the synchronous phase angles of the two parts. Therefore, we need a PLL system that has both fast response and stable

control for varying grid voltages. Fig. 2 shows a block diagram of a three-phase PLL system.

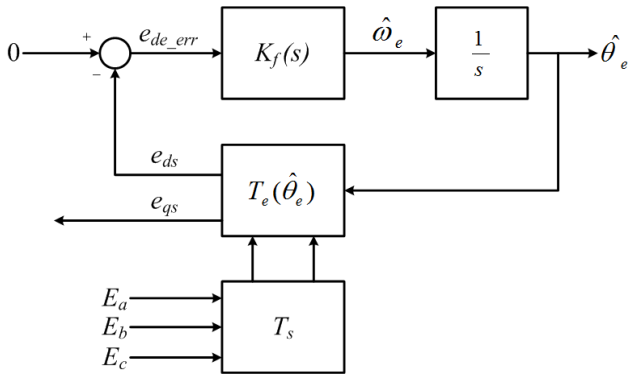

Fig. 2. Three-phase PLL system.

2.2 Unbalanced and distorted grid voltage

When the grid voltage is unbalanced, a power ripple that is twice the line frequency occurs because of the negative sequence elements. This ripple results from a distortion of the DC-link voltage. It reduces the reliability and stability of the system. Thus, we must reduce the power ripple via control of the unbalanced current.

The voltage at the point of common coupling (PCC) of a distributed system is likely to be distorted by harmonic currents due to the nonlinear load. The output currents of grid-connected inverter systems can be distorted by low-order harmonics because of the grid voltage distortion. Fig. 3(a) shows a harmonic current source made by a distorted voltage (e_h), and Fig. 3(b) presents the compensation of the harmonic currents achieved by injecting the voltage (v_{sh}) to offset the harmonic elements in the grid voltage.

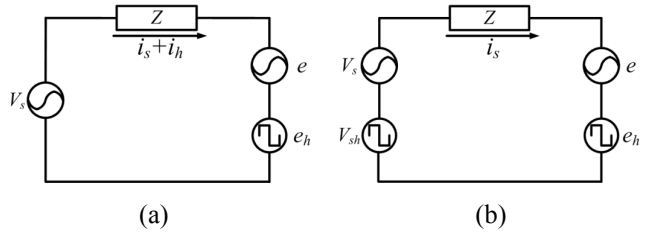

(a) (b)

Fig. 3. The per-phase equivalent circuit of grid side under the distorted source voltage: (a) before; (b) after the compensation [14].

2.3 Novel grid-connected inverter

Fig. 4 shows a block diagram of a grid-connected inverter using a PR current controller and a PR harmonic compensator. If imbalance and distortion occur in the grid voltage, the PR controller controls each phase current to reduce the power ripple and compensate for low-order harmonics such as the third, fifth, and seventh harmonics in the output current.

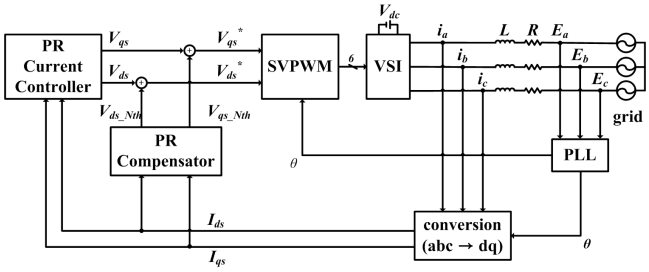

Fig. 4. A block diagram of a grid-connected inverter using PR controllers.

3. Control of grid-connected inverter system using PR controller

The PR controller is used in the stationary frame. In contrast to the PI controller used in the synchronous frame, the computation sequence of the PR controller is shortened because there is no transforming frame from the stationary frame to synchronous frame as in PI controller. It is possible to replace the PI controller in the synchronous frame with the PR controller in the stationary frame. This frequency-modulating process can be mathematically expressed as:

$$G_{AC}(s) = G_{DC}(s - j\omega) + G_{DC}(s + j\omega) \tag{1}$$

where $G_{AC}(s)$ represents the equivalent stationary-frame transfer function [9]. Therefore, for the ideal and nonideal integrators of $G_{DC}(s) = K_i/s$ and $G_{DC}(s) = K_i/(1+(s/\omega_c))$, where K_i represents the controller gain and $\omega_c << \omega$ represents the cutoff frequency, the derived AC integrators $G_{AC}(s)$ are expressed as [10, 11]:

$$G_{AC}(s) = \frac{Y(s)}{E(s)} = \frac{2K_i s}{s^2 + \omega^2} \tag{2}$$

$$G_{AC}(s) = \frac{Y(s)}{E(s)} = \frac{2K_i(\omega_c s + {\omega_c}^2)}{s^2 + 2\omega_c s + ({\omega_c}^2 + \omega^2)} \approx \frac{2K_i(\omega_c s + {\omega_c}^2)}{s^2 + 2\omega_c s + \omega^2} \tag{3}$$

When a proportional term K_p is added to (2), it represents the ideal PR controller with an infinite gain at the frequency of ω (see Fig. 5(a)) but at no other frequencies. K_p is tuned in the same way as the PI controller, which determines the dynamics of the system in terms of the bandwidth, phase, and gain margin. To solve the stability problems of infinite gain, it is possible to take (3) instead of (2) to give a nonideal PR controller, as shown in Fig. 5(b). Although its gain is finite, it is still relatively high in order to give a small steady-state error.

Another difference between (3) and (2) is that in (3) the bandwidth can be widened by tuning ω_c appropriately. This reduces the sensitivity to the slight frequency variation that occurs in a typical grid [12, 13].

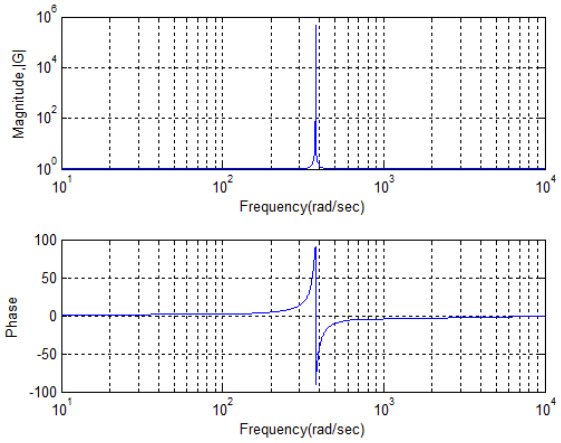

(a)

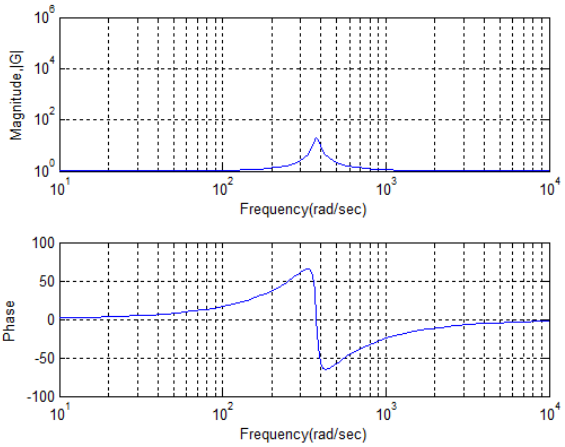

(b)

Fig. 5. Bode plots of (a) ideal; (b) nonideal PR compensators; K_p=1, K_i=20, ω=377rad/s, and ω_c=10rad/s.

3.1 Power ripple reduction

Fig. 6 shows a conventional method for reducing power ripple under unbalanced grid conditions. The dual-controller uses four PI controllers to control the positive-negative sequence elements of active and reactive currents. Fig. 7 shows our method for reducing power ripple; it uses the PR controller in the stationary frame. The control inputs of our controller are the active-reactive currents of the stationary frame. Because these reference currents are found by summing the reference currents of the positive and negative elements, just one PR controller is needed to control the power ripple.

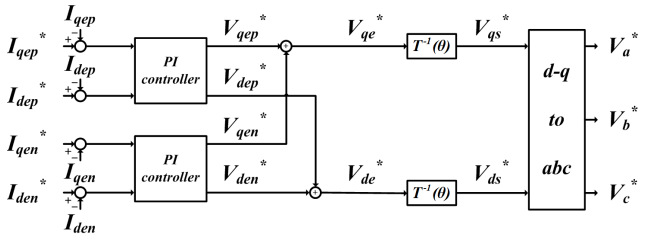

Fig. 6. Reduction of power ripple using PI controllers.

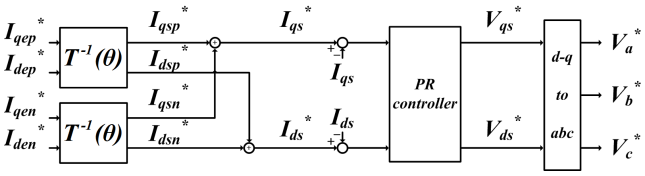

Fig. 7. Reduction of power ripple using PR controllers.

3.2 Compensation of distorted grid voltage using PR controller

Fig. 8 shows a block diagram of a harmonic compensator with a PI controller. In this figure, the harmonics are caused by the distorted grid voltage.

The currents of the stationary frame are synchronized by multiplying them with the positive and negative values of the harmonic orders: ±3, ±5, and ±7. This is done using the phase angle from the PLL of the grid-side voltage, and this involves extracting the positive and negative harmonic elements. Subsequently, the third, fifth, and seventh harmonic currents of the synchronous frame are extracted by using the low-pass filter, and the extracted currents are controlled to zero with the PI controller. Fig. 8 shows that the computational burden is proportional to the harmonic order [14].

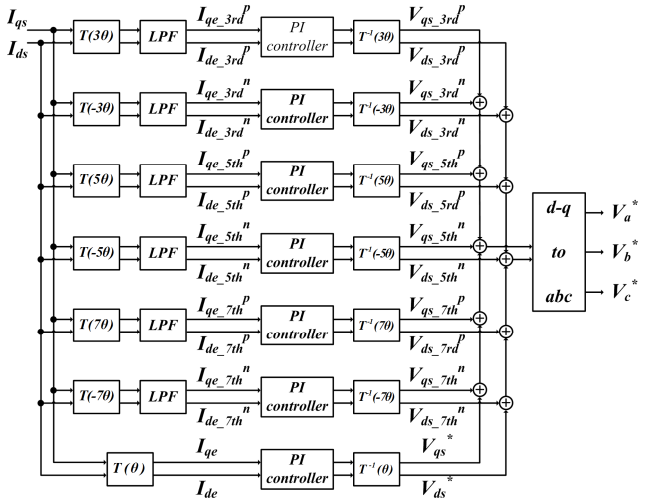

Fig. 8. Block diagram of harmonic compensator using PI controllers to eliminate the 3rd, 5th, and 7th harmonic currents.

In contrast, it is possible to compensate for the harmonics using the PR controller, which has a relatively high gain in a specific frequency band. We can compensate for the harmonics selectively by adjusting the frequency of the low-order harmonics that we wish to eliminate. As an example, the transfer functions of an ideal and a non-ideal harmonic compensator (HC) are designed to compensate for the third, fifth, and seventh harmonics. These harmonics are the most prominent in a typical current spectrum, and the compensators are [8]:

$$G_h(s) = \sum_{h=3,5,7} \frac{2K_{ih}s}{s^2 + (h\omega)^2} \tag{4}$$

$$G_h(s) = \sum_{h=3,5,7} \frac{2K_{ih}\omega_c s}{s^2 + 2\omega_c s + (h\omega)^2} \tag{5}$$

where h is the harmonic order to compensate for, and K_{ih} represents the individual resonant gain.

Fig. 9 shows a block diagram of our approach for the elimination of low-order harmonics using the PR controller. We also use a PI controller to compare our method with the conventional approach.

The existing technique for the compensation of harmonic distortion requires a cumbersome operation to transform the frame of each harmonic order. However, using the PR controller simplifies the method as the number of PR compensators needed corresponds to the harmonic order. It is easy to compensate for the harmonic currents using this technique.

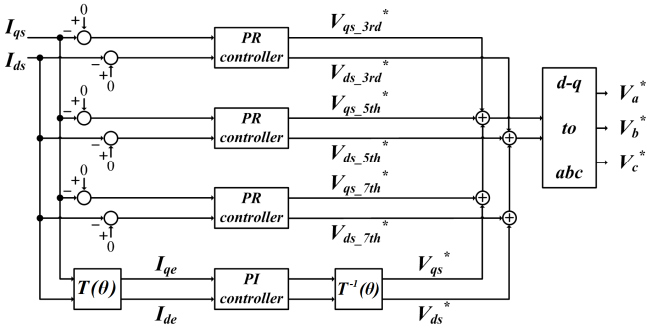

Fig. 9. Compensation for 3rd, 5th, and 7th harmonics using PR controllers.

4. Simulations

We perform simulations to confirm the validity of our algorithm. The simulation parameters for the grid-connected inverter system are given in Table 1.

Table 1. Simulation parameters

DC-link voltage	600V
DC-link capacitance	4500uF
Control period	100us
Grid phase voltage	311.127V
Frequency	60Hz

We investigate the validity of our algorithm for both unbalanced and distorted grid voltage. These waveforms are shown in Fig. 10, where the imbalance factor is 18.18%, and the total harmonic distortion (THD) ratio is approximately 5%.

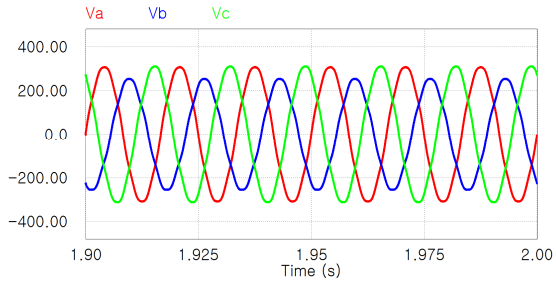

Fig. 10. Unbalanced and distorted grid voltage.

Fig. 11 shows the power wave before the power ripple reduction and the harmonic compensation. Because of the unbalanced grid voltage, the power wave contains a 120 [Hz] ripple component.

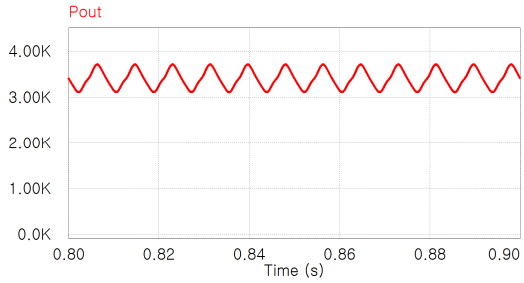

Fig. 11. Power wave before power ripple reduction and harmonic compensation.

Fig. 12 shows the three-phase currents under the same conditions as in Fig. 11. Thus, the three-phase currents are balanced under the conditions, and represented non-sinusoidal waveform due to the harmonics.

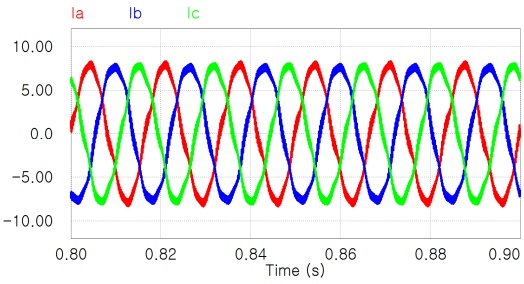

Fig. 12. Three-phase currents before power ripple reduction and harmonic compensation.

Fig. 13 shows the power wave with our method for the reduction of the power ripple and the harmonics. Via the imbalance control, we reduce the 120 [Hz] ripple component in the power, and we also compensate for the harmonics.

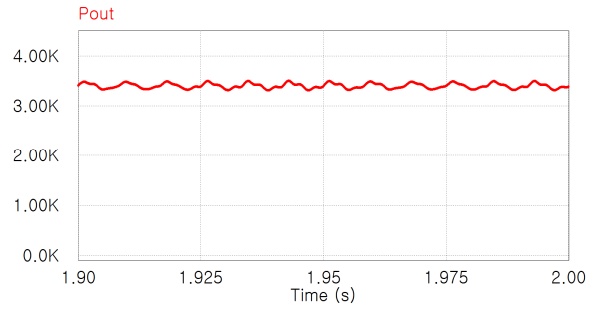

Fig. 13. Power wave after power ripple reduction and harmonic compensation.

Fig. 14 shows the three-phase currents after the power ripple reduction and harmonic compensation. Henceforth, the three-phase currents become unbalanced and display the sinusoidal waveform due to the harmonic compensation.

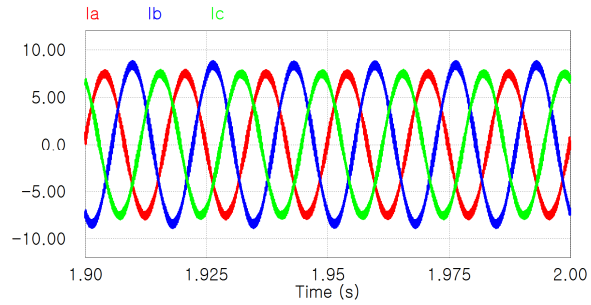

Fig. 14. Three-phase currents after power ripple reduction and harmonic compensation.

5. The experimental results

We apply our technique to a 10-kW grid-connected inverter system. Fig. 15 shows the digital controller based on a digital signal processor (TMS320F28335).

Fig. 16 shows the unbalanced and distorted grid voltage where the imbalance factor is 18.18% as in the simulation, and the third, fifth, and seventh harmonic components are 2%.

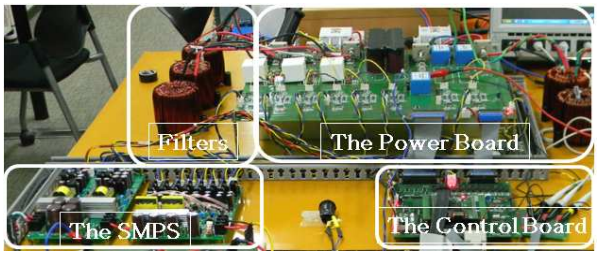

Fig. 15. Experimental setup.

Fig. 17 shows the three-phase currents and the power wave without the power ripple reduction and harmonic compensation. As the grid voltage is unbalanced and affected by the harmonics, it can be seen that the power

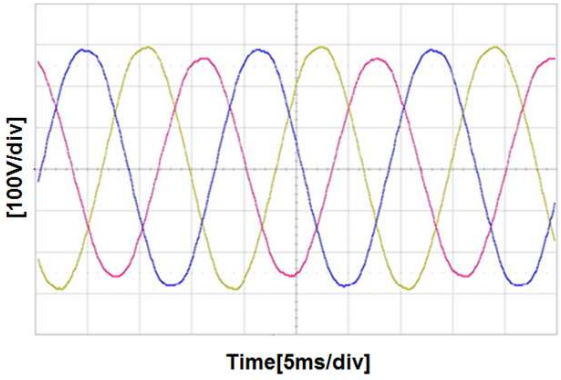

Fig. 16. Unbalanced and distorted grid voltage.

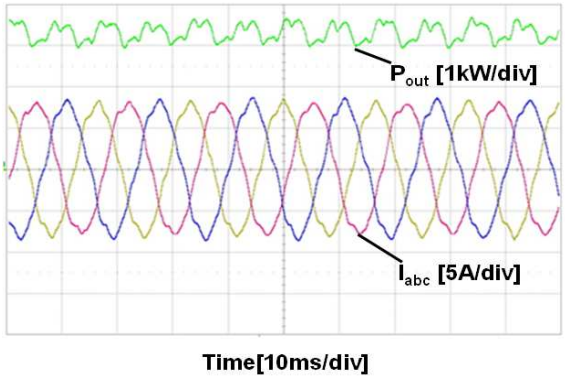

Fig. 17. Three-phase currents and power wave before power ripple reduction and harmonic compensation.

wave contains 120 [Hz] ripple components and various harmonics. In contrast to the simulation results, the power wave has not only third, fifth, and seventh harmonic components but also other harmonics because of the sampling frequency. The three-phase currents are distorted by many harmonics in the balanced state.

Fig. 18 shows the three-phase currents and the power wave when only the unbalanced current control is applied. Although the ripples of the power wave are reduced by the

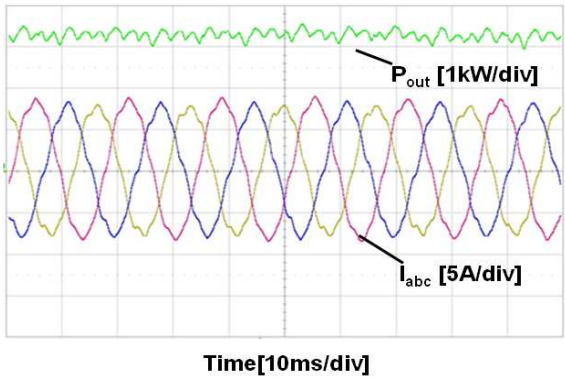

Fig. 18. Three-phase currents and power wave only when power ripple reduction is applied.

power ripple reduction, the ripples still remain due to other harmonics. It is possible to check that the three-phase currents waveform is unbalance controlled in order to reduce the power ripple. However, because of the harmonic compensation not being applied the three phase current waveform can be verified to be non-sinusoidal.

Fig. 19 shows the three-phase currents and the power wave when only the harmonic compensation is applied. The harmonic compensation makes the three-phase currents close to a sinusoidal wave, which has no third, fifth, or seventh harmonics. We compensate for the harmonics in the power wave. Thus, the power wave becomes similar to a sinusoidal wave with 120 [Hz] components.

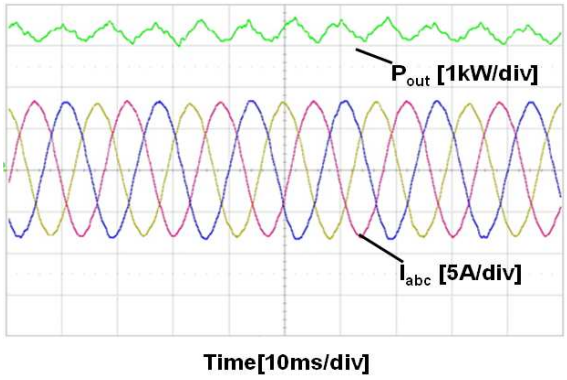

Fig. 19. Three-phase currents and power wave only when harmonic compensation is applied.

Fig. 20 shows the three-phase currents and the power wave after the power ripple reduction and harmonic compensation. The distortion of the three-phase currents is compensated for by eliminating the third, fifth, and seventh harmonic elements. The power ripple reduction and the harmonic compensation reduce the ripple of the 120 [Hz] elements and the harmonics in the power wave. The power ripple is reduced by 40% when both techniques are used.

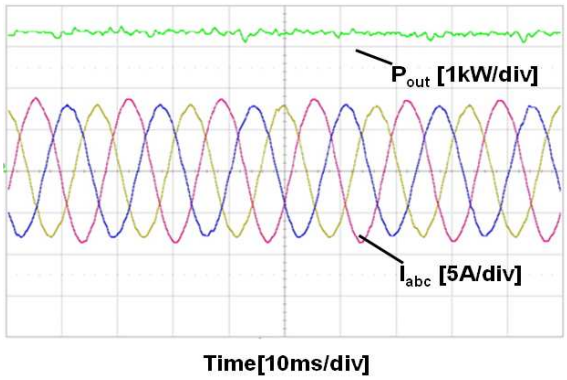

Fig. 20. Three-phase currents and power wave after power ripple reduction and harmonic compensation.

Figs. 21 and 22 show the FFT form of the *a*-phase current before and after the harmonic compensation. It can be seen that the third, fifth, and seventh harmonics have been compensated.

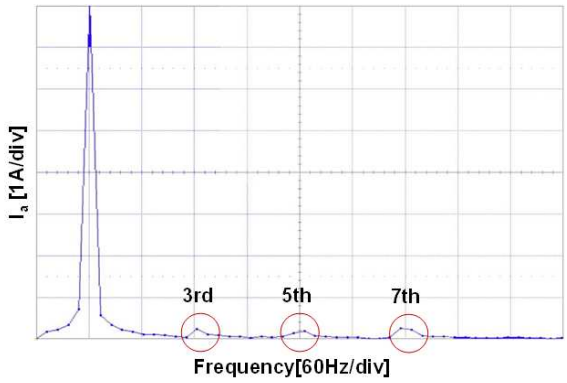

Fig. 21. FFT form of *a*-phase current before harmonic compensation.

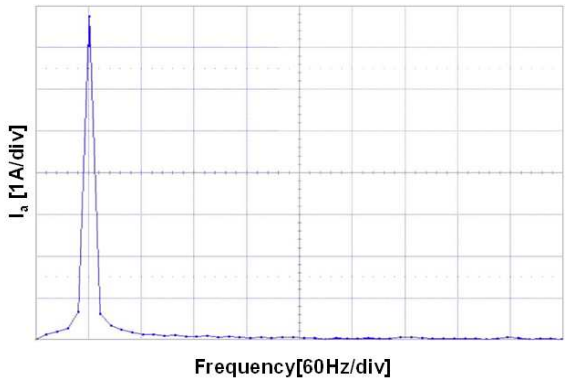

Fig. 22. FFT form of *a*-phase current after harmonic compensation.

Fig. 23 shows the THD spectrum of the *a*-phase current. Because the harmonic compensation is done for only the third, fifth, and seventh harmonics, the THD is calculated for only these harmonics. With the compensation for the distortion, the THD factor has been reduced by 3.78%.

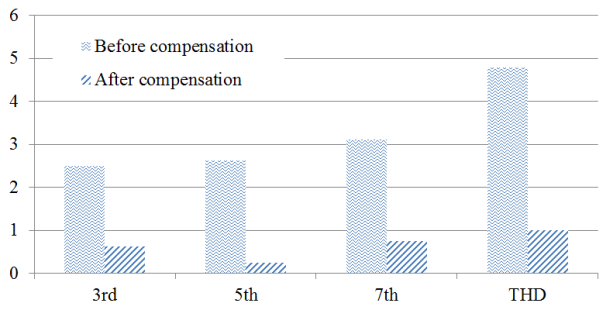

Fig. 23. THD spectrum of *a*-phase current.

6. Conclusion

We have presented a control scheme for unbalanced current that provides power stability under an unbalanced grid voltage and a method to compensate for harmonic distortion using a PR controller. We use just one PR controllers whereas two PI controllers are needed in the conventional approach. Using a PR compensator for the harmonic distortion simplifies the complex computation. We have experimented with a 10-kW system. The simulated and experimental results confirm the feasibility and effectiveness of our PR controller.

Acknowledgements

This work was supported by the Human Resources Development of the Korea Institute of Energy Technology Evaluation and Planning (KETEP) grant funded by the Korea government Ministry of Knowledge Economy (No. 20114010203030).

This work was supported by KETEP (20111020400030-11-1-000) which is funded by MKE (Ministry of Knowledge Economy).

References

[1] R. J. Wai, W. H. Wang, and C. Y. Lin, "High-performance Stand-Alone Photovoltaic Generation System", *IEEE Transactions on Industrial Electronics*, vol. 55, no. 1, pp. 240-250, Jan. 2008.

[2] S. R. Bull, "Renewable Energy Today and Tomorrow", *in Proceedings of the IEEE*, vol. 89, no. 8, pp. 1216-1226, Aug. 2001.

[3] S. Rahman, "Green Power" What Is It and Where Can We Find It?", *IEEE Power and Energy Magazine*, vol. 1, no. 1, pp. 30-37, Jan/Feb. 2003.

[4] S. -K. Chung, "Phase-locked loop for grid-connected three-phase power conversion system", *in Proceedings of the IEE Electric Power Applications*, vol. 147, no. 3, pp. 213-219, May. 2000.

[5] S. Alepuz, S. Busquets-Monge, J. Bordonau, J. Gago, D. Gonzalez, and J. Balcells, " Interfacing Renewable Energy Sources to the Utility Grid Using a Three-Level Inverter", *IEEE Transactions on Industrial Electronics*, vol. 53, no. 5, pp. 1504-1511, Oct. 2006.

[6] J. J. Negroni, C. Meza, D. Biel, and F. Guinjoan, "Control of a Buck Inverter for Grid-Connected PV Systems: a Digital and Sliding Mode control Approach", *in Proceedings of the IEEE International Symposium on Industrial Electronics*, pp. 739-744. Jun. 2005.

[7] G. Shen, X. Zhu, J. Zhang, and D. Xu, "A New feedback Method for PR Current Control of LCL-filter-Based Grid-Connected Inverter", *IEEE Transactions on Industrial Electronics*, vol. 57, no. 6, pp. 2033-2041, Jun. 2010.

[8] R. Teodorescu, F. Blaabjerg, M. Liserre, and P. C. Loh, "Proportional-resonant controllers and filters for grid-connected voltage-source converters", *in Proceedings of the IEE Electric Power Applications*, vol. 153, no. 5, pp. 750-762, Sept. 2006.

[9] P. C. Tan, P. C. Loh, and D. G. Holmes, "High performance harmonic extraction algorithm for a 25kV traction power quality conditioner", *in Proceedings of the IEE Electric Power Applications*, vol. 151, no. 5, pp. 505-512, Sept. 2004.

[10] D. N. Zmood and D. G. Holmes, "Stationary Frame current Regulation of PWM Inverter with Zero Steady-State Error", *IEEE Transactions on Power Electronics*, vol. 18, no. 3, pp. 814-822, May. 2003.

[11] G. Xiaoqiang, Z. Qinglin, and W. Weiyang, "A Single-Phase Grid-Connected Inverter System with Zero Steady-State Error", *in Proceedings of the IEEE Power Electronics and Motion Control Conference*, vol. 1, pp. 1-5, Aug. 2006.

[12] S. Fukuda, and T. Yoda, "A Novel Current-tracking Method for Active Filters Based on a sinusoidal internal Model", *IEEE Transactions on Industry Applications*, vol. 37, no. 3, pp. 888-895, May/Jun. 2001.

[13] M. Liserre, R. Teodorescu, and F. Blaabjerg, "Stability of Photovoltaic and Wind Turbine Grid-connected Inverters for a Large Set of Grid impedance Values", *IEEE Transactions on Power Electronics*, vol. 21, no. 1, pp. 263-272, Jan. 2006.

[14] J. I. Jang, and D. C. Lee, "High Performance Control of Three-Phase PWM Converters under non-ideal Source Voltage", *in Proceedings of the IEEE International Conference on Industrial Technology*, pp. 2791-2796, Dec. 2006.

Jong-Hyun Lee He was born in Jeonju, Korea, in 1985. He received the B.S. degree in Electrical and Computer Engineering from Ajou University, Suwon, Korea, in 2011. He is currently working toward the M.S. degree at Ajou University, Suwon, Korea. His research interests are power conversion and electric machine drives.

Hae-Gwang Jeong He was born in Jeonju, Korea, in 1982. He received the B.S. degree in Electrical Engineering from Chonbuk National University, Jeonju, Korea, in 2008. He received the M.S. degrees in the Department of Electrical and Computer Engineering from Ajou University. He is currently working toward the Ph.D. degree at Ajou University. His research interests are power conversion and electric machine drives.

Kyo-Beum Lee He was born in Seoul, Korea, in 1972. He received the B.S. and M.S. degrees in Electrical and Electronic Engineering from the Ajou University, Korea, in 1997 and 1999, respectively. He received the Ph.D. degree in electrical engineering from the Korea University, Korea in 2003. From 2003 to 2006, he was with the Institute of Energy Technology, Aalborg University, Aalborg, Denmark. From 2006 to 2007, he was with the Division of Electronics and Information Engineering, Chonbuk National University, Jeonju, Korea. In 2007 he joined the Department of Electrical and Computer Engineering, Ajou University, Suwon, Korea. He is an associated editor of the IEEE Transactions on Power Electronics, the IEEE Transactions on Industrial Electronics, and the Journal of Power Electronics. He has received two IEEE prize paper awards. His research interests include electric machine drives, renewable power generations, and electric vehicles.